ISSN 0967-0912, Steel in Translation, 2018, Vol. 48, No. 11, pp. 732–736. © Allerton Press, Inc., 2018.
Original Russian Text © S.M. Tleugabulov, Zh.V. Eremeeva, M.B. Kurmanseitov, 2018, published in Stal', 2018, No. 11, pp. 2–6.

Carburization and Decarburization in Iron and Steel Production

S. M. Tleugabulov[a], *, Zh. V. Eremeeva[b], and M. B. Kurmanseitov[a]

[a] *Satpaev Kazakhstan National Technical University, Almaty, Kazakhstan*
[b] *Moscow Institute of Steel and Alloys, Moscow, Russia*
**e-mail: suleiman_70@mail.ru*

Received November 7, 2018

Abstract—The development of small-scale iron production has expanded the output of cast products in Russia. It is often necessary to strengthen the surface of cast-iron components. To that end, special alloys and metallic powders are applied to the working surface. In addition, strengthening by decarburization in the solid state offers a short cut from the ore to the final iron component; it is even more efficient than the familiar path from ore to steel. In the present work, such structural conversion of cast-iron components is considered. Experiments are conducted in two stages: (1) production and preparation of cast-iron blanks from industrial waste; (2) solid-state decarburization of the cast-iron blanks. The initial iron source consists of rolling scale and iron oxide formed in the surface etching of rolled sheet at AO ArcelorMittal Temirtau. Analysis of the microstructure and the change in the mass transfer between the cast-iron plate and the applied layer of oxide powder yields consistent results and indicates that solid-state decarburization of cast iron and finished cast-iron components is feasible.

Keywords: iron, cast iron, steel, ore, coal, carbon, reduction, smelting, solidification, decarburization, metal structure

DOI: 10.3103/S0967091218110116

Iron and carbon are the most common elements on the planet and so serve as the basic resources in metallurgy. The extraction and use of iron ore and coal provides the basis for one of the most important human activities: iron and steel production. Today, 80% of the global output of iron and steel is produced in the system consisting of a blast furnace and an oxygen converter, using coke [1].

The stable development of the iron and steel industry and its prospects depend on the efficiency of the blast-furnace process. Iron-ore pieces and selected coke are the basic components of the blast-furnace batch. The complex heat and mass transfer in the working space of the blast furnace begins with the injection of hot blast through the tuyeres around the circumference of the hearth (the furnace's lower section), where incomplete combustion of the coke and fuel forms hot reducing gas at 2000–2200°C. The hot reducing gas, containing CO, H_2, and N_2, transmits heat and acts as a reducing agent: it is responsible for heating of the batch column, reduction of the iron, melting of the reduced batch, the formation of iron and slag melt, and its discharge through the furnace mouth at an average temperature of 200°C. As we see, the thermal efficiency in the blast furnace is high (90%). In addition, the blast-furnace gas produced is used (after purification) as fuel for heating the arc and is injected at the bottom of the furnace. In this closed cycle, all the input and output parameters are fixed, monitored, and used to control the processes [2].

Coke plays an important role, not only as a generator of thermal energy and reducing gases but also as coke packing in the furnace's high-temperature zone, maintaining the opposing flows of molten batch and hot reducing gas. Filtration of the slag and metal melt through this packing ensures complete reduction of the metal and its carburization by the solid carbon in the coke. The composition of the slag and metal melt is practically completed here. Therefore, after filtration through the coke bed, the blast-furnace slag has a low content of unreduced metals (no more than 1.0%) in comparison with the slag in other metallurgical processes. The unavoidable carburization of iron in the blast furnace, which is a highly efficient and highly productive system, ends with the discharge of ferrocarbon alloy melt (hot metal), containing 4.2–4.5% C. Then the hot metal passes to oxygen converters for oxidative processing, with the goal of decarburization and steel production. As we see, carburization and decarburization of the ferrocarbon melt are integral to traditional iron and steel production. The iron and steel have distinctive characteristics in the molten and solid state.

Steel is widely used in manufacturing on account of its viscoplasticity, deformability and strength (after appropriate treatment). Cast iron is hard and brittle, which limits its use in the construction industry and

Table 1. Composition of batch components, wt %

Component	Fe_{tot}	Fe	MnO	SiO_2	Al_2O_3	CaO	S	P	C
Rolling scale	67.65	28.25	0.24	—	—	—	0.017	0.02	—
Iron oxide	68.0	—	—	—	—	—	0.02	0.03	—
Charcoal	—	—	–	1.65	0.62	0.2	0.37	—	95

elsewhere. The production of cast-iron components and machine parts is expanding because of the benefits of iron: it is readily fusible and flows well when molten. In addition, the mechanical characteristics of cast iron are largely determined by the structural transformations of the carbon present. To improve the structural characteristics of cast iron, the production of high-strength cast iron by conversion of the graphite from plate to ball structure under the action of special modifiers is currently under development [3, 4]. High-strength iron with globular graphite is characterized by yield point and tensile strength higher than in steel and relatively high elastic modulus. The fluidity of the melt and high strength of the cast iron permit expansion in the range of iron products [5]. The production of foundry iron with good plasticity and forging plasticity is also under development: this process depends on motion and structural transformation of the graphite in the iron under the influence of heating and modifiers [6, 7]. The size of the graphite structures is decreased, and the iron takes on pearlitic structure, characterized by ductility and plasticity. The formation of malleable iron is also facilitated by partial transfer of the dissolved carbon through the outer surface of the cast iron on account of reaction with oxide components. That accelerates the formation of small graphite structures.

Such structural transformations of the ferrocarbon alloy and its conversion to construction materials meeting manufacturing requirements are associated primarily with motion and transformation of the carbon, which has high atomic mobility. The radius of the carbon atom (0.077 E) is markedly less than that of iron (0.127 E). Therefore, it penetrates easily into the crystal lattice of iron through the interatomic gaps. On penetrating into the λ Fe structure, it forms a solution corresponding to ferrite phase. On dissolving in γ Fe, it forms austenite phase. In addition, it forms a chemical compounds with iron: cementite Fe_3C, in which the carbon concentration is 6.67%.

The carbon concentration in ferrite is 0.025–0.10%, depending on the temperature. In austenite, as in the interstitial solid solution in γ Fe, the carbon concentration reaches 2.14% at 1147°C and 0.8% at 727°C. On cooling the hot metal from the blast furnace, solid structures consisting mainly of a solution of cementite in austenite are formed. We also note the appearance of ledeburite (mean concentration 4.2–4.5%). As is evident, carbon, which is present in the hot metal in solution and as chemical compounds, is highly mobile and active. Therefore, in discussing its redox properties, it is expedient to simply refer to dissolved carbon.

The activity of the dissolved carbon in the ferrocarbon alloy shows that it is preferable to free carbon in coal or coke as a reducing agent in solid-phase processes [8, 9]. Therefore, the decarburization of carbon may be organized not only by oxidative remelting in an oxygen converter but also in the solid state, with qualitative transformations not in the melt but in the final cast-iron products.

The development of small-scale iron production has expanded the output of cast products in Russia. It is often necessary to strengthen the surface of cast-iron components. To that end, special alloys and metallic powders are applied to the working surface [10, 11]. An alternative is strengthening by decarburization in the solid state [12].

Strengthening of cast components and machine parts by decarburization in the solid state offers a short cut from the ore to the final iron component; it is even more efficient than the familiar path from ore to steel. In the present work, we consider such structural conversion of cast-iron components.

Experiments are conducted in two stages: (1) production and preparation of cast-iron blanks from industrial waste; (2) solid-state decarburization of the cast-iron blanks. The initial iron source consists of rolling scale and iron oxide formed in the surface etching of rolled sheet by acid at AO ArcelorMittal Temirtau. Table 1 presents the chemical composition of the components employed.

BATCH PREPARATION AND IRON-INGOT PRODUCTION

As we see in Table 1, the total iron concentration in the scale is 67.65%. Of that total, 21.95% comes from wustite FeO (whose content is 28.25%), while the remaining 45.70% is provided by hematite Fe_2O_3. In addition, the scale includes a small amount of MnO. The total quantity of oxygen that may be released as gas from the iron and magnesium oxides is determined from an equation taking account of the degree of reduction of iron ($R_{Fe} = 0.98$) and manganese ($R_{Mn} = 0.75$)

$$g_0 = 10^{-2}[\mathrm{Fe}_{(h)} \times .3276 + \mathrm{Fe}_{(w)} \times 0.2296 + 0.5812\mathrm{MnO}], \quad \text{kg/kg of scale.} \tag{1}$$

Table 2. Composition of metal ingots, wt %

Sample	[C]	[Si]	[Mn]	[S]	[P]
From scale	4.25	0.15	1.23	0.03	0.02
From iron oxide	4.38	0.10	—	0.032	0.01

Here $Fe_{(h)}$ and $Fe_{(w)}$ are the iron concentrations in hematite and wustite, respectively, %.

We see in Table 1 that iron oxide, the second batch component, does not contain FeO. The oxide consists entirely of hematite Fe_2O_3, and the total quantity of oxygen that may be released as gas is determined from the equation

$$O_{Fe} = 10^2 \times 0.3276 \times Fe_{(h)},\ \text{kg/kg of iron oxide.} \quad (2)$$

Substituting the numerical values into Eqs. (1) and (2), we find that the total quantity of oxygen that may be released as gas from the scale is

$$g_0 = 0.2015\ \text{kg/kg of scale.}$$

Likewise, from Eq. (2), the total quantity of oxygen that may be released as gas from the iron oxide

$$O_{Fe} = 0.2247,\ \text{kg/kg of iron oxide.}$$

Such oxygen is gasified in reductive roasting. Solid carbon is selected as the reducing agent.

By successive phase transformation of the metal oxides, the stoichiometric consumption of solid carbon in the reduction of metals corresponding to 0.152 kg/kg of scale and 0.17 kg/kg of iron oxide may be determined [13].

The metal yield is 0.67 and 0.6769 kg/kg from the scale and iron oxide, respectively. The carbon consumption in the carburization of this metal is 0.029 and 0.030 kg/kg, respectively. The total carbon consumption in the reduction and carburization of the metal is 0.181 and 0.200 kg/kg, respectively. Converting to charcoal, the corresponding figures are 0.172 and 0.210 kg/kg. On that basis, we formulate two batches:

(1) rolling scale (0.85 kg/kg of batch) + charcoal (0.15 kg/kg of batch);

(2) iron oxide (0.83 kg/kg of batch) + charcoal (0.17 kg/kg of batch).

From each batch, 250-g samples are prepared for the experimental melts. After crushing to piece size ≤1.0 mm, each sample of ore–coal batch is loaded in a Tamman furnace. The system is slowly heated (at 8–10°C/min) to 900°C and then at 12°C/min to 1500°C. At that temperature, the reduction of the metal is complete and hot metal is formed. After holding for 20 min, the melt is cast in a refractory tray of rectangular cross section. After cooling to room temperature, the metal component of the melt is separated from the slag and its surface is machined. We obtain ingots of mass 139.0 and 141 g from the first and second batch samples, respectively. Table 2 presents the chemical composition of the metal samples.

As is evident, the ingots consist of cast iron. After surface machining, the cast-iron plates are cut into sections, and plane samples (width 30 mm, length 50.0 mm, and thickness 5 mm) are produced.

SOLID-STATE DECARBURIZATION OF CAST-IRON BLANKS

The flat cast-iron blanks (of mass 68 and 70 g) are placed in a boat of rectangular cross section and covered with iron-ore powder (mainly FeO). The boat is placed in a sealed cell within the reaction zone of a Nabertherm RHTC 80-230/15/B410 pipe furnace. The temperature of the system is increased at 12–15°C/min to 1100°C and held for 60, 70, 80, and 90 min. At 1000°C, gas is released thanks to solid-state reaction between dissolved carbon and iron oxide from the oxide powder

$$FeO + [C] = Fe_{met} + CO. \quad (3)$$

The reduced iron at the contact surface of the cast-iron plate is converted to solid solution. In other words, the following substitution occurs

$$Fe_3C + FeO = 4Fe + CO\uparrow. \quad (4)$$

Slow diffusional reaction is observed. The gas released per unit time is so small that its composition cannot easily be monitored on a gas analyzer. Therefore, the mass transfer at the contact surface is quantitatively assessed by measuring the mass of the cast-iron plate and the oxide powder before and after the experiment. At the end of each experiment, the mass of the hot metal and oxide powder is recorded. The change in mass of the cast-iron plate is due to the reactions in Eqs. (3) and (4) . In other words, the mass of the plate falls on account of the gasification of dissolved carbon in Eq. (3), while the mass increases on account of reaction of the reduced iron by Eq. (4). Since the atomic mass of iron is 4.66 times that of carbon, the resultant mass increase is the difference between the gain in iron mass and the consumption of dissolved carbon. The mass fraction of consumed carbon [C] associated with the increase in plate mass is determined from the equation

$$\Delta g_{[C]} = \frac{m_C}{m_{Fe} - m_C}\Delta g, \quad (5)$$

where Δg is the mass difference of the cast iron at the beginning and end of the experiment, g; m_C is the atomic mass of carbon (12 g); and m_{Fe} is the atomic mass of iron (56 g).

Since $m_C/(m_{Fe} - m_C) = 12/(56 - 12) = 0.273$, we may rewrite Eq. (5) in the form

$$\Delta g_{[C]} = 0.273\Delta g.$$

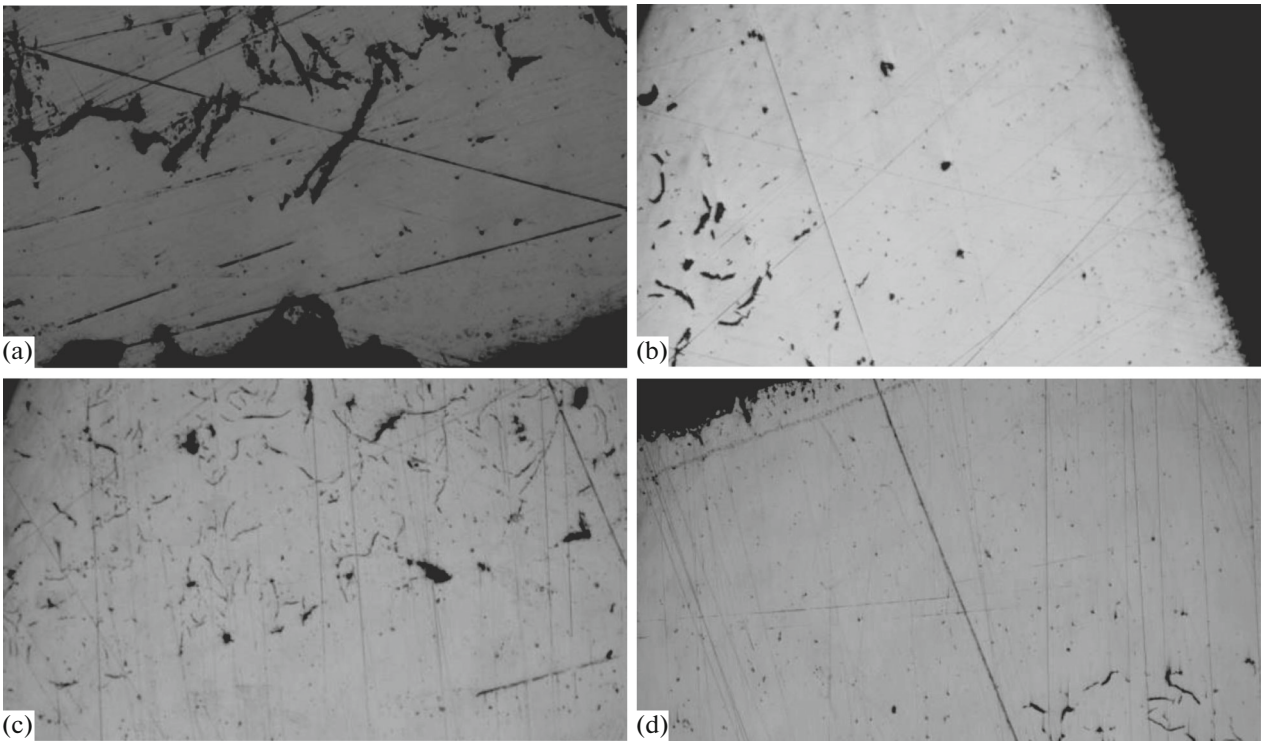

Fig. 1. Structure of cast-iron plates after holding for 60 (a), 70 (b), 80 (c), and 90 (d) min at 1100°C.

The mass of the layer of oxide powder decreases solely on account of the reduction of iron from FeO by the dissolved carbon, in accordance with Eq. (3). Accordingly, the mass loss of the powder may be expressed in the form

$$\Delta g_{ox} = \frac{m_{FeO}}{m_C}\Delta g_{[C]} = \frac{72}{12}\Delta g_{[C]} = 6\Delta g_{[C]}. \quad (6)$$

Measurement of the mass of the plate and the applied powder permits the determination of the following:

—the mass increase Δg of the plate, g;

—the mass decrease Δg_{ox} of the oxide powder, g.

The mass decrease Δg_{ox} of the oxide powder agrees with the mass increase Δg of the plate. The mass of dissolved carbon consumed in reduction of the metal from the oxide powder is derived from $\Delta g_{[C]}$ in Eq. (5): 0.37–0.80 g, depending on the holding time. However, the depth of decarburization remains to be established. To that end, we determine the microstructure of the plate cross section in another experiment. First, the plate cross section is ground. The metal samples are observed on a JSM 5910 electron microscope: the boundaries of the decarburized layer are identified in different cross sections. In Fig. 1, we show the structure of the plates at 1100°C, with holding for 60, 70, 80, and 90 min. The structural transformation of the surface layer is evident, as well as the increase in thickness of the decarburized layer with increase in the holding time.

It is clear from Fig. 1 that the solid-state decarburization of the iron in the plate's surface layers is successful. In addition, we can track the progress of decarburization into the depth of the plate as holding at the specified temperature continues. The mean thickness of the decarburized layer is 1.5 mm after 60 min and 2.8 mm after 90 min. Accordingly, to assess the degree of decarburization $\Delta R_{[C]}$ and the mean residual carbon concentration, we assume that the mean thickness of the decarburized layer is 2.2 mm.

We determine the degree of decarburization of the plate's surface layer as the ratio of the mass loss $\Delta g_{[C]}$ and the total mass $g_{[C]}$ of dissolved carbon in a surface layer of thickness 2.2 mm: $\Delta R_{[C]} = \Delta g_{[C]}/g_{[C]}$.

The mean residual concentration of dissolved carbon is determined from the equation

$$\Delta[C] = [C](1 - \Delta R_{[C]}),$$

where $\Delta[C]$ is the initial carbon concentration in the plate, %.

Table 3 presents the characteristics of solid-state decarburization of the iron plates.

We see that microstructural data agree with the change in mass transfer between the cast-iron plate and the oxide powder. That indicates that solid-state

Table 3. Characteristics of solid-state decarburization of the surface layer of iron plates at 1100°C

Initial mass of cast-iron plate, g	Decarburization characteristic	Holding time, min			
		60	70	80	90
68.0	Δg, g	1.35	1.92	2.34	2.85
	$\Delta g_{[ox]}$, g	–2.208	–3.144	–3.84	–4.68
	$\Delta g_{[C]}$, g	0.368	0.524	0.64	0.78
	$\Delta R_{[C]}$, fraction	0.32	0.448	0.556	0.676
	Δ[C], %	2.81	2.32	1.79	1.36
70.0	Δg, g	1.45	1.98	2.49	3.01
	$\Delta g_{[ox]}$, g	–2.37	–3.24	–4.08	–4.93
	$\Delta g_{[C]}$, g	0.396	0.54	0.68	0.822
	$\Delta R_{[C]}$, fraction	0.33	0.45	0.56	0.68
	Δ[C], %	2.73	2.31	1.84	1.32

decarburization of cast iron and finished cast-iron components is feasible.

CONCLUSIONS

Decarburization is accompanied by structural transformation of the iron to steel in the surface layer. Thus, the effects of the carburization in the cast iron and solid-state decarburization of the iron are complementary and have a net positive effect.

Iron is fluid and permits the production of parts of any shape. Its deficiencies are brittleness and poor weldability. These deficiencies are countered by decarburization of the working surfaces and conversion of the surface layer to steel under the oxide coating. This short route from hot metal to the final product provides clear economic and environmental benefits.

REFERENCES

1. Kurunov, I.F., The direct production of iron and alternatives to the blast furnace in iron metallurgy for the 21st century, *Metallurgist*, 2010, vol. 54, nos. 5–6, pp. 335–342.
2. Tleugabulov, S.M., Nosov, K.G., Uryupin, S.D., and Shidlovskii, A.A., *Upravlenie protsessom smeshannogo vosstanovleniya zheleza v shakhte domennoi pechi* (Control of Mixed Reduction of Iron in Blast Furnace), Alma-Ata: Gylym, 1991.
3. Chaikin, V.A., Ishutin, V.V., and Chaikina, N.V., Production of high-strength cast iron, *Trudy Vos'mogo s"ezda liteishchikov Rossii* (Proc. Eight Congr. of Foundry Workers of Russia), Rostov-on-Don, 2007, vol. 1, pp. 61–63.
4. Trukhov, A.P. and Malysrov, A.I., Production technology of high-strength cast iron with nodular graphite, in *Liteinye splavy i plavka* (Foundry Alloys and Smelting), Moscow: Akademiya, 2004, pp. 28–32.
5. Marshirov, I.V., Mustafin, G.A., Moskalev, V.G., et al., Production of high-strength cast iron with nodular graphite for castings of agricultural machinery, *Polzunovskii Al'm.*, 2008, no. 3, pp. 203–204.
6. Girshovich, N.G., *Chugunnoe lit'e* (Iron Casting), Moscow: Gos. Nauchno-Tekh. Izd. Chern. Tsvetn. Metall., 1978.
7. Pronman, I.M., Shalashov, V.V., and Berger, A.Kh., USSR Inventor's Certificate no. 142670, *Byull. Izobret.*, 1964, no. 22.
8. Ryzhonkov, D.I. and Tomlyanovich, V.D., *Teoriya metallurgicheskikh protsessov. Kineticheskie zaonomernosti vosstanovleniya okisnykh materialov v sloe* (Theory of Metallurgical Processes: Kinetics of Reduction of Oxidized Materials in a Layer), Moscow: Mosk. Inst. Stali Splavov, 1981.
9. Tleugabulov, S.M., Abikov, S.B., and Koishina, G.M., Solid phase recovery of refractory metals, *XIV Int. Sci. Congr. "Machines. Technologies. Materials," Varna, Bulgaria, September 13–16, 2017*, Sofia: Sci. Tech. Union Mech. Eng., 2017, no. 4, vol. 4, pp. 296–297.
10. Mochul'ski, L. and Andersen, E.B., RF Patent 2235805, *Byull. Izobret.*, 2003, no. 27.
11. Londarskii, A.F., Moskvitin, G.V., Mel'shanov, A.F., et al., RF Patent 2621088, *Byull. Izobret.*, 2017, no. 16.
12. Tleugabulov, S.M., Koishina, G.M., Sultamurat, G.M., and Tazhiev, E.B., RF Patent 28558, *Byull. Izobret.*, 2014, no. 6.
13. Tleugabulov, S.M., *Teoreticheskie osnovy polucheniya metallov, splavov i perspektivnykh materialov: uchebnoe posobie dlya vuzov* (Theory of Production of Metals, Alloys, and Advanced Materials: Manual for Higher Education Institutions), Almaty: Red. Izd. Kom. Ucheb. Metod. Lit., 2001.

Translated by Bernard Gilbert